Barrier-to-autointegration factor is required to segregate and enclose chromosomes within the nuclear envelope and assemble the nuclear lamina

Ayelet Margalit*, Miriam Segura-Totten[†‡], Yosef Gruenbaum*, and Katherine L. Wilson[†§]

*Department of Genetics, Institute of Life Sciences, Hebrew University of Jerusalem, Givat Ram, Jerusalem 91904, Israel; and [†]Department of Cell Biology, Johns Hopkins University School of Medicine, 725 North Wolfe Street, Baltimore, MD 21205

Edited by Roger D. Kornberg, Stanford University School of Medicine, Stanford, CA, and approved January 19, 2005 (received for review November 10, 2004)

Barrier-to-autointegration factor (BAF) binds dsDNA, LEM-domain proteins, and lamins. *Caenorhabditis elegans* BAF requires Ce-lamin and two LEM-domain proteins (Ce-emerin and Ce-MAN1) to localize during nuclear assembly. It was unknown whether Ce-lamin and LEM proteins, in turn, depend on Ce-BAF (mutually dependent structural roles). RNA interference-mediated down-regulation of Ce-BAF caused gross defects in chromosome segregation, chromatin decondensation, and mitotic progression as early as the two-cell stage, and embryos died at the ≈100-cell stage. Nuclear pores reassembled, whereas Ce-lamin, Ce-emerin, and Ce-MAN1 bound chromatin but remained patchy and disorganized. The nuclear membranes formed but failed to enclose anaphase-bridged chromatin. Time-lapse imaging showed two phenotypes: anaphase-bridged chromatin that eventually resolved, and segregated chromatin that returned to the midzone. Thus, the assembly of BAF, lamins, and LEM-domain proteins is mutually dependent, and is required to capture segregated chromosomes within the nascent nuclear envelope. Embryos that escaped lethality by down-regulation of Ce-BAF grew into sterile adults with misplaced distal tip cells and gonads, further suggesting that mild postembryonic reductions in BAF disrupt tissue-specific functions.

nuclear assembly | emerin | LEM domain | distal tip cell | nuclear organization

Barrier-to-autointegration factor (BAF) is a small (10 kDa) dsDNA-binding protein highly conserved among metazoans (1). BAF also binds LEM-domain nuclear proteins, lamins, and homeodomain transcription activators (2). The human LEM-domain gene family includes LAP2, emerin, MAN1, and four proposed members: Lem2 (NET-25), Lem3, Lem4, and Lem5 (3). LEM-domain proteins share a defining motif, the LEM-domain, which mediates direct binding to BAF (4, 5). LEM-domain proteins influence many activities, including nuclear assembly, gene expression, DNA replication, actin dynamics, and signaling downstream of the TGF-β family (6). BAF directly binds and represses the activity of Crx and related homeodomain transcription factors *in vivo* (7). BAF also competes with a repressor, germ cell-less, for binding to emerin *in vitro* (8). Thus, BAF might influence gene expression at multiple levels. Additional roles for BAF in nuclear structure are suggested by its direct binding to nuclear lamins (8), which form stable filaments in metazoan nuclei. Lamins determine nuclear shape and mechanical stability and support essential functions, including DNA replication and polymerase II-dependent transcription (9, 10).

BAF, lamins, and LEM-domain proteins appear to have a special relationship. Each can directly bind the other; for example, emerin can form stable three-way complexes with BAF and lamin A (8). Similarly, BAF binds directly to lamins and to all tested LEM-domain proteins (2). Interestingly GFP-BAF is highly mobile in living cells, but nevertheless interacts detectably and directly with emerin *in vivo* (11), suggesting BAF interacts dynamically with lamins and LEM-domain proteins.

Caenorhabditis elegans is a relatively simple metazoan that encodes BAF (Ce-BAF), one B-type lamin (Ce-lamin), and three LEM-domain proteins. Two (Ce-emerin and Ce-MAN1) are integral proteins of the nuclear inner membrane, whereas the third (Ce-Lem3) has no transmembrane domain (12). Ce-MAN1 is homologous to human MAN1, but orthologous to human Lem2 (3). *C. elegans* provides a powerful *in vivo* system in which to study interactions between BAF, lamin, and LEM-domain proteins (12–16), particularly in the context of nuclear assembly and disassembly during embryogenesis. Ce-lamin is essential for viability, as shown by RNA interference (RNAi)-mediated down-regulation (14). Ce-BAF was suggested to be essential (16). In each case, the phenotype includes defective chromosome segregation during mitosis, apparently anaphase-bridged chromatin, aneuploidy, and death by the 100-cell stage. In cells depleted of Ce-lamin, the other partners (Ce-emerin, Ce-MAN1, and Ce-BAF) all fail to assemble around chromatin (14, 15). Similarly in cells codepleted of two LEM-domain proteins (Ce-emerin and Ce-MAN1), postmitotic reassembly of Ce-lamin and Ce-BAF is defective (15). These findings suggested two mutually exclusive models for BAF function during mitosis. In the first model, assembly of Ce-BAF into reforming nuclei depends on Ce-lamin and LEM-domain proteins. This dependent model predicts that Ce-lamin and LEM-domain proteins would assemble normally in cells that lack Ce-BAF. The alternative mutually-dependent model predicts that Ce-lamin and Ce-emerin would both fail to assemble properly in cells that lack Ce-BAF. To test these models, we characterized the RNAi-mediated down-regulation phenotype for Ce-BAF. Our results confirm that Ce-BAF is essential for *C. elegans* embryogenesis. Furthermore our findings strongly support the mutually-dependent structural model for BAF function during mitosis, and reveal that loss of Ce-BAF destabilizes the segregated status of daughter chromosomes.

Materials and Methods

***C. elegans* Strains.** *C. elegans* N2 strain was obtained from the *C. elegans* Genome Center and cultured as described (17). *C. elegans* line AZ212 expressing GFP fused to histone H2B (H2B-GFP) was a kind gift from J. Austin (University of Chicago, Chicago). Strain JK2049, which expresses GFP driven by the distal tip cell (DTC)-specific *lag-2* promoter, was con-

This paper was submitted directly (Track II) to the PNAS office.

Abbreviations: BAF, barrier-to-autointegration factor; RNAi, RNA interference; Ce, *Caenorhabditis elegans*; DIC, differential interference contrast microscopy; DTC, distal tip cell; NPC, nuclear pore complex.

[‡]Present address: Department of Science and Technology, Universidad Metropolitana, P.O. Box 21150, San Juan, Puerto Rico 00928.

[§]To whom correspondence should be addressed. E-mail: klwilson@jhmi.edu.

www.pnas.org/cgi/doi/10.1073/pnas.0408364102

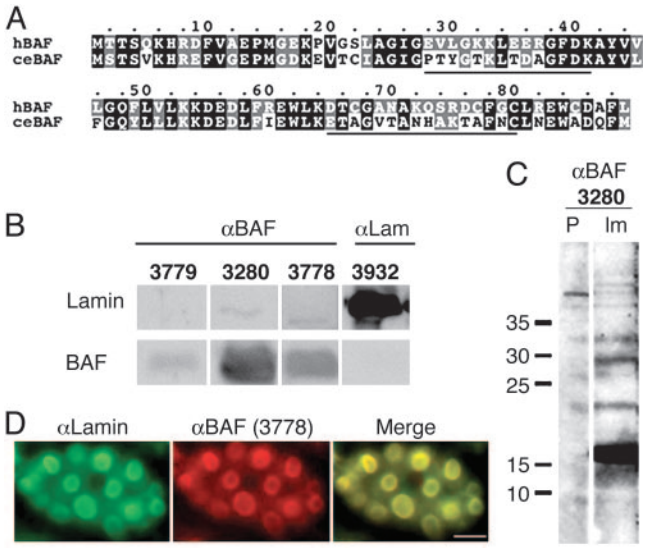

Fig. 1. Abs against Ce-BAF. (*A*) Amino acid sequences of human BAF (hBAF) and *C. elegans* BAF (ce-BAF). Identical and similar amino acids are shaded black and gray, respectively. Black lines indicate residues 28–41 of Ce-BAF (the peptide antigen for sera 3778 and 3280) and residues 65–80 (antigen for serum 3779). (*B*) Immunoblots of similar amounts of bacterially expressed Ce-lamin (*Upper*) or Ce-BAF (*Bottom*), both of which were solubilized with 8 M urea before loading on the gel (see *Materials and Methods*), probed with immune serum 3778, 3779, or 3280 against Ce-BAF (αBAF), or serum 3932 against Ce-lamin (αLam). (*C*) Western blot of crude protein extract of mixed-stage *C. elegans* animals probed with preimmune (P) or immune (I) serum 3280. (*D*) Indirect immunofluorescence staining of wild-type *C. elegans* embryos with Abs against endogenous Ce-lamin (green), endogenous Ce-BAF (serum 3778, red), and merged signals (merge). (Scale bar, 10 μm.)

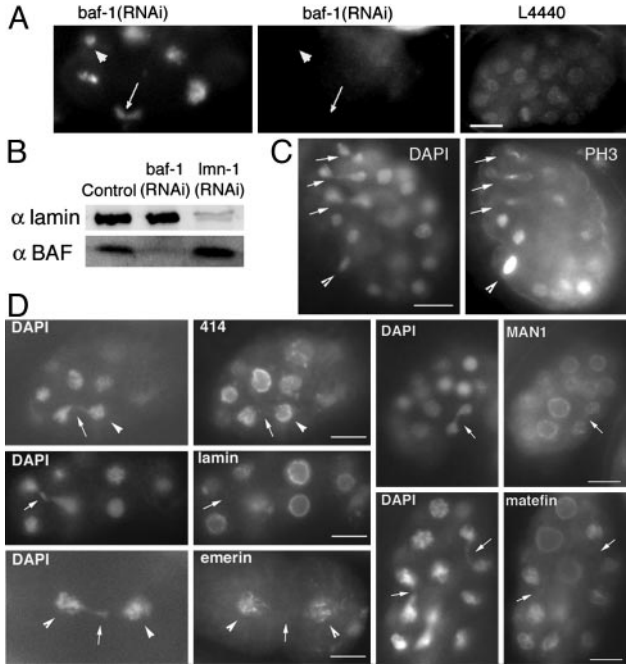

Fig. 2. Localization of nuclear envelope markers in bridged versus segregated chromatin in *baf-1*(*RNAi*) embryos. (*A*) Ce-BAF protein was successfully depleted in *baf-1*(*RNAi*) embryos. Indirect immunofluorescence staining with serum 3779, which localizes endogenous Ce-BAF in the nucleus of embryos from worms fed empty L4440 vector (*Right*). (*Left*) A *baf-1*(*RNAi*) embryo stained with DAPI for DNA (*Left*) and Ce-BAF (*Center*); the Ce-BAF protein signal was significantly reduced. Arrowhead indicates a nucleus with unusually condensed chromatin. Arrow indicates anaphase-bridged chromatin. (Bar, 10 μm.) (*B*) Immunoblots of protein lysates from *baf-1*(*RNAi*) embryos, *lmn-1*(*RNAi*) embryos, or embryos from wild-type worms fed with L4440 empty vector (control) were probed with Abs against Ce-lamin (*Upper*) or Ce-BAF (serum 3280; *Lower*). Ce-lamin protein levels were unaffected, whereas Ce-BAF was ≈10% of its normal level in *baf-1*(*RNAi*) embryos. (*C*) Mitotic phosphorylation persists on anaphase-bridged chromatin. A typical *baf-1*(*RNAi*) embryo double-stained with DAPI (to visualize DNA) and Abs against a mitotic phosphoepitope on histone H3 (PH3). Arrowhead indicates normal metaphase chromosomes in a mitotic cell. Arrows indicate three different pairs of segregated chromatin, each connected by bridged chromatin. PH3 stains the bridged chromatin, but not the segregated chromatin. (Bar, 10 μm.) (*D*) Embryos DAPI-stained to visualize DNA, and stained by indirect immunofluorescence using Abs against one of the following endogenous proteins: nucleoporins (mAb 414), Ce-lamin, Ce-emerin, Ce-MAN1, or matefin. Arrows point to the anaphase-bridged chromatin that connects two segregated chromatin masses. Arrowheads in the 414- and emerin-stained images indicate one or both (respectively) of the corresponding masses of segregated chromatin. (Bars, 10 μm.)

structed by J. Kimble (University of Wisconsin, Madison) and obtained from the *C. elegans* Genome Center.

Abs, Indirect Immunofluorescent Staining, and Immunoblots. Adult *C. elegans* were fixed and prepared for staining by indirect immunofluorescence as described (12). Rat anti-Ce-BAF sera 3778 and 3779 were used at 1:100 dilution for indirect immunofluorescence. Rabbit anti-Ce-BAF serum 3280 was used at 1:1,000 dilution for immunoblots. Sera 3778 (15) and 3280 were raised against a peptide antigen, comprising residues 28–41 of Ce-BAF. Serum 3779 was raised against a synthetic keyhole limpet hemocyanin-conjugated peptide comprising residues 65–80 of Ce-BAF (ETAGVTANHAKTAFNC). BAF serum 3778 was affinity-purified by binding the BAF peptide (Reduce-Imm reducing kit and sulfolink kit, Pierce) and used undiluted for indirect immunofluorescence; other sera were diluted at 1:50 [rat anti-Ce-emerin serum 3598; (13)], at 1:400 [affinity-purified rabbit anti-Ce-lamin Abs, (14)], at 1:100 [rat anti-Ce-MAN1 serum 3597 (13)], or at 1:100 [rat anti-matefin serum 3663 (18)]. Phosphohistone H3 Abs (Upstate Group, Waltham, MA) and mAb 414 against nucleoporins (Babco, Richmond, CA) were used at 1:100 dilution. Secondary Cy3-conjugated goat anti-rat or anti-rabbit Abs and FITC-conjugated goat anti-rat or anti-rabbit Abs (Jackson ImmunoResearch) were used at 1:200 dilution.

For immunoblotting, proteins were resolved by SDS/PAGE (15% acrylamide), then transferred and probed with the indicated anti-Ce-BAF serum (1:1,000 dilution) or serum 3932 against Ce-lamin (1:10,000 dilution). For Fig. 1*B*, His-tagged Ce-BAF (in the pET28a vector) and Ce-lamin (in the pET20 vector) proteins were expressed in bacteria, solubilized by treatment with 8 M urea, and purified on Ni^{2+}-NTA-agarose (Qiagen, Valencia, CA) before loading gels. For Fig. 2*B*, *baf-1*(*RNAi*) and control worms were collected from three 50-mm Petri dishes ≈56 h after feeding, washed with M9 buffer, treated for 5 min with hypochlorite solution (1.1% hypochlorite and 0.62 M NaOH), then washed with M9, and the embryos were collected. For protein lysates, the embryos were mixed with 30 μl of 2× sample loading buffer (100 mM Tris·HCl, pH 6.8/20% glycerol/200 mM DTT/4% SDS/0.2% Bromophenol blue), frozen in liquid nitrogen, and then boiled for 10 min.

Microscopy and Live-Cell Imaging. Transmission electron microscopy of *C. elegans* embryos was performed essentially as described (19); the fixative consisted of 2.5% freshly made paraformaldehyde and 2.5% EM-grade glutaraldehyde (Agar Scientific, Essex, U.K.) in 0.1 M Na-Hepes, pH 7.0. Immunostained embryos and cells were imaged by using a Zeiss Axioplan II microscope equipped for fluorescence. For live cell imaging, an Axiocam charge-coupled device camera and the AxioVision

image analysis package were used to record time-lapse data every 2 or 1.5 min.

RNAi-Mediated Experiments. *baf-1* complete cDNA was subcloned into feeding vector L4440 and used for RNAi feeding at 16°C as described (18). Control animals were fed with bacteria carrying an empty L4440 construct. Worms were either examined live for viability and GFP fluorescence, or fixed and stained for indirect immunofluorescence.

Results

C. elegans and human BAF are 52% identical (Fig. 1*A*). We raised two independent polyclonal sera (3778 and 3280) against Ce-BAF residues 28–41, and one serum (3779) against Ce-BAF residues 65–80 (Fig. 1*A*; see *Materials and Methods*). All three sera recognized recombinant Ce-BAF on immunoblots (Fig. 1*B Lower*), although the serum 3779 signal was weak. None cross-reacted with recombinant Ce-lamin (Fig. 1*B Upper*). Immunoblot analysis of whole worm lysates revealed a major 17-kDa band (Fig. 1*C* shows results for serum 3280). This band was not recognized by preimmune serum (Fig. 1*C*), was competed by treatment with the antigenic peptide (data not shown), and was therefore specific. Serum 3280, which was best for immunoblots, gave weak signals by indirect immunofluorescence (data not shown). Serum 3778 decorated the nuclear envelope and nuclear interior during interphase (Fig. 1*D*), colocalized with Ce-lamin (Fig. 1*D*; see also ref. 15), and dynamically changed its localization during mitosis by becoming more punctate, localizing near condensing chromatin, and remaining chromatin-associated through telophase (Fig. 6, which is published as supporting information on the PNAS web site). Serum 3779, which recognizes a different epitope on Ce-BAF, also stained the nucleus, but the envelope signal was much weaker (Fig. 2*A*).

Ce-BAF Is Essential and Has Roles in Chromosome Segregation. A previous RNAi study suggested Ce-BAF was essential (16), but lacked controls for the efficiency of down-regulation. To rigorously determine the loss of function phenotype for Ce-BAF, we used RNAi-mediated interference to down-regulate *baf-1* in *C. elegans* embryos. Endogenous Ce-BAF protein was significantly depleted, as shown by the faint residual signal in *baf-1*(*RNAi*) embryos stained with serum 3779 [Fig. 2*A*, *baf-1*(*RNAi*)], compared with the nuclear signals in control embryos fed empty vector (Fig. 2*A*, L4440). Depletion of Ce-BAF protein was independently confirmed by staining embryos with serum 3778 (data not shown). Down-regulation was further confirmed by immunoblotting equal amounts of lysate proteins with serum 3280, the most sensitive Ab on immunoblots, showing ≈90% reduced levels of Ce-BAF, but not Ce-lamin, in protein lysates from *baf-1*(*RNAi*) embryos (Fig. 2*B*, middle lane) compared with untreated worms (Fig. 2*B*, control). Ce-BAF protein levels were not reduced in cells lacking Ce-lamin [Fig. 2*B*, *lmn-1*(*RNAi*)]. Thus, neither protein requires the other for its expression or stability. Loss of Ce-BAF was lethal, because *baf-1*(*RNAi*) embryos did not progress past the 100-cell stage. Two major phenotypes were detected: abnormally condensed chromatin in interphase nuclei (Fig. 2*A*, arrowhead) and anaphase-bridged chromatin (Fig. 2*A*, arrow). These results confirmed the chromosome segregation defect reported by Zheng *et al.* (16), and further showed that Ce-BAF influences chromatin structure in interphase nuclei (aberrant chromatin condensation). To further characterize the phenotypes of Ce-BAF-depleted mitotic cells, we used anaphase-bridged chromatin as a marker in the studies below.

In a previous study of cells down-regulated for both Ce-emerin and Ce-MAN1, the anaphase-bridged chromatin retained a mitosis-specific phosphorylated form of histone H3 long after the neighboring segregated chromatin lost this marker (15). We wondered whether the same anomaly was caused by loss of Ce-BAF. Controls verified that Abs against the phosphohistone H3 epitope gave strong signals on mitotic chromosomes in *baf-1*(*RNAi*) embryos [Fig. 2*C Right* (PH3), arrowhead] as expected. Interestingly, these Abs also preferentially recognized anaphase-bridged chromatin, but not segregated chromatin [Fig. 2*C Right* (PH3), arrows]. We do not understand why mitotic modifications persist on the anaphase-bridged chromatin. However, because this phenotype can result either from loss of Ce-BAF (this work) or loss of its LEM-partners (15), these proteins might coassemble structures, or comediate pathway(s), that ensure efficient progression through mitosis. Consistent with this interpretation, down-regulation of Ce-BAF also increased the time spent in mitosis; for example, control cells progressed rapidly from prophase to telophase (2 min), whereas >5 min elapsed in *baf-1*(*RNAi*) cells (data not shown; see below).

To further characterize the anaphase-bridged chromatin, we used specific Abs to localize five endogenous nuclear envelope markers: nucleoporins (the subset recognized by mAb 414), Ce-lamin, Ce-emerin, Ce-MAN1, and matefin [a lamin-binding SUN-domain protein of the inner nuclear membrane (18)]. Except for potentially dim punctate staining of nucleoporins (Fig. 2*D*, 414, arrow), these markers were not detected on bridged chromatin (Fig. 2*D*, arrow in images stained for lamin, emerin, MAN1, or matefin). We attributed this result to persistent mitotic phosphorylation of the bridged chromatin (Fig. 2*C*), which would be expected to locally block nuclear envelope assembly.

To test the mutually-dependent structural model, we examined the two masses of segregated chromatin connected by each bridge, to determine whether any marker proteins had assembled into a nuclear rim at the chromatin surface. As internal controls for nuclear envelope rim localization, we found a subset of embryos in which neighboring interphase cells still showed nuclear envelope rim staining. These neighboring cells were presumably not yet fully BAF-depleted, because in the majority of embryos stained at the most potent window of *baf-1*(*RNAi*), Ce-lamin rim organization was lost in interphase cells (data not shown). In *baf-1*(*RNAi*) embryos with interphase rim staining, examination of cells with bridged chromatin showed that Ce-lamin, Ce-emerin, Ce-MAN1, and matefin all associated with the chromatin surface, but remained patchy and failed to assemble into a coherent nuclear rim pattern (Fig. 2*D*, see arrowheads in emerin-stained embryo). In contrast, the subset of nucleoporins recognized by mAb 414 reassembled into a wrinkled but obviously rim-like pattern on the segregated chromatin (Fig. 2*D*, 414, arrowhead). This result suggested that nuclear membranes were present and nuclear pore complexes (NPCs) had formed (as confirmed below). Indeed, Ce-lamin is required to space, not assemble, NPCs (14). Thus, depletion of Ce-BAF profoundly disrupted the postmitotic assembly of Ce-lamin and three lamin-binding membrane proteins, strongly supporting mutually dependent structural roles for Ce-BAF, Ce-lamin, and LEM-domain proteins during nuclear assembly.

Chromosome Segregation Is Unstable in BAF-Depleted Cells. We were puzzled why all cells did not arrest with anaphase-bridged chromatin. We therefore used time-lapse microscopy to image living *baf-1*(*RNAi*) embryos as they progressed through mitosis. For these experiments, the RNAi construct was fed to *C. elegans* animals that stably expressed H2B-GFP, allowing direct visualization of chromosomes in living cells (Fig. 3) (20). Anaphase-bridged chromatin was detected as early as the two-cell (Fig. 2*D*, emerin staining) and four-cell (Fig. 3*A*) stages. Differential interference contrast microscopy (DIC) imaging suggested that many daughter cells with bridged chromatin could complete cytokinesis (Fig. 3*A Middle* and *Bottom*). Live imaging further suggested that the segregation defect differed qualitatively between cells, perhaps because the levels of

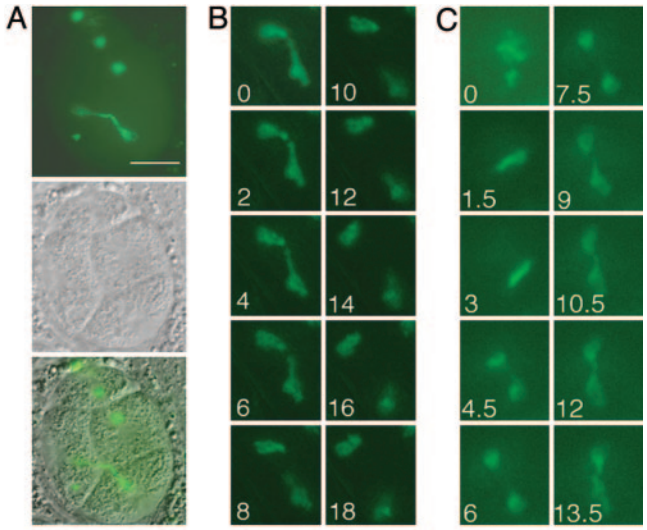

Fig. 3. Dynamic behavior of bridged chromatin in *baf-1*(*RNAi*) embryos. (*A–C*) Adult *C. elegans* stably expressing H2B-GFP were fed bacteria expressing Ce-BAF dsRNA. (Bar, 10 μm.) (*A*) Corresponding H2B-GFP (*Top*), DIC (*Middle*), and merged H2B-GFP/DIC images (*Bottom*) of a four-cell embryo; daughter cells underwent cytokinesis despite the presence of bridged chromatin. (*B*) Time-lapse images of H2B-GFP in a living embryo recorded at 2-min intervals starting after the bridge formed; the apparently bridged chromatin eventually resolved into the daughter nuclei. (*C*) Time-lapse images of H2B-GFP in a living embryo recorded at 1.5-min intervals starting at prometaphase (0 min), where chromosome condensation was nonuniform. After an apparently normal metaphase (1.5–3 min), most chromatin segregated (4.5–7.5 min), but later returned to the midzone (10.5–13.5 min; see text).

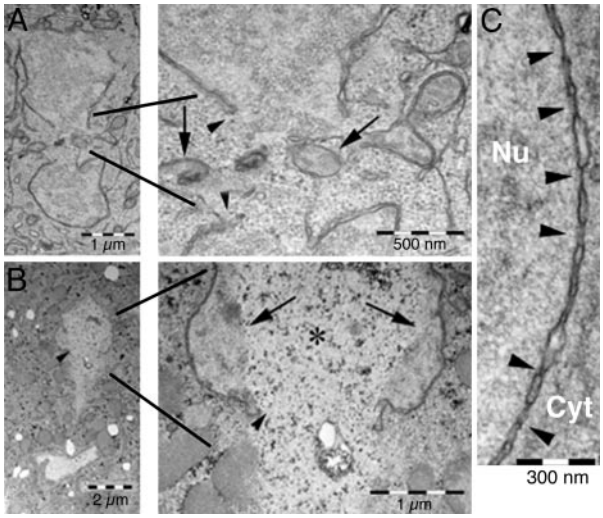

Fig. 4. Nuclear morphology in *baf-1*(*RNAi*) embryos. Visualization of *baf-1*(*RNAi*) embryos by thin-section transmission electron microscopy. (*A* and *B*) Images on the left and right represent low- and high-magnification views, respectively, of the region indicated by black lines. Most nuclei had a large gap in their nuclear envelope (gap edges indicated by arrowheads in *A* and *B*), presumably where bridged chromatin was located. Arrows in *A* indicate mitochondria near the bridged chromatin. Arrows in *B* indicate the boundary between central chromatin and more condensed peripheral chromatin. (*B Right*) Asterisk indicates chromatin similar in appearance to the bridged chromatin. (*C*) High-magnification view of segregated chromatin in a *baf-1*(*RNAi*) embryo reveals closely spaced NPCs (arrowheads). Scale bars are marked in each image. Nu, nucleoplasm; cyt, cytoplasm.

Ce-BAF dropped below a critical threshold(s) at different times. For example, Fig. 3*B* shows daughter cells recorded at 2-min intervals after the chromatin bridged. At later stages, the bridged chromatin appeared to resolve by incorporation into the daughter nuclei (Fig. 3*B*, 8–12 min). We cannot strictly eliminate the possibility that this resolution was an artifact of photobleaching. However, arguing against this artifact, we also saw the opposite phenotype (see below); furthermore, the proportion of cells in which bridged chromatin resolved was higher during early embryonic divisions (data not shown), possibly because residual levels of maternal Ce-BAF were sufficient to slowly rescue the bridged chromatin. The second chromatin phenotype is shown in Fig. 3*C*, recorded at 1.5-min intervals starting when chromatin was condensing, at prometaphase. Condensation appeared abnormal (nonuniform; note two distinct masses of chromatin in Fig. 3*C*, time 0), but resulted in an apparently normal metaphase (Fig. 3*C*, 1.5–3 min). In early anaphase, only a trace of bridged chromatin was visible (Fig. 3*C*, 4.5 and 6 min). Remarkably, during the next 4 min, a large fraction of the seemingly segregated chromatin failed to remain in the nascent nucleus, and returned to the midzone (Fig. 3*C*, 9–13.5 min) and stayed in the midzone for at least 5 min more (data not shown). Of 27 total cells examined during the most potent window of *baf-1*(*RNAi*), 11 cells (40%) resolved the chromatin bridge, and 15 cells (55%) collapsed back to the midzone and did not segregate normally during the ensuing 25 min. Normal chromosome segregation was seen in only one cell (5%). These phenotypes suggest that Ce-BAF, or the lamina network that mutually coassembles with Ce-BAF, or both, are needed to stabilize or capture the segregated chromosomes within nascent nuclei.

BAF-Depleted Daughter Nuclear Membranes Fail to Fully Enclose Chromatin, Potentially Allowing Segregated Chromatin to Escape. The apparent assembly of nucleoporins into nascent nuclei in *baf-1*(*RNAi*) cells (Fig. 2*D*) suggested but did not prove that nuclear membranes and NPCs were present. We therefore fixed and thin-sectioned *baf-1*(*RNAi*) embryos and used EM to visualize any nuclear membranes or NPCs (Fig. 4). High magnification revealed many typical NPC profiles on segregated chromatin masses (Fig. 4*C*, arrowheads). Large regions of segregated chromatin were bordered by two nuclear membranes (Fig. 4 *A* and *B*, see also *Supporting Text* and Fig. 7, which are published as supporting information on the PNAS web site), demonstrating that Ce-BAF depletion did not grossly disrupt membrane targeting to the segregated chromatin, or membrane fusion. However, two striking phenotypes were observed: heterogeneously condensed chromatin, and a large gap where the nuclear envelope failed to associate with segregated chromatin. This gap was detected in at least 62% of nuclei imaged ($n = 125$), and this percentage was a minimum because nuclei that appeared ungapped in these sections might have revealed gaps in different sections. In controls fed empty L4440 vector ($n = 130$), all nuclei were fully enclosed (data not shown). Most gaps, indicated by arrowheads in Figs. 4*A* and 7, correlated with bridged chromatin, suggesting that Ce-BAF is somehow required to (*i*) complete segregation, (*ii*) maintain segregation, or (*iii*) capture segregating chromatin within the nascent envelope. Abnormally condensed chromatin was detected in 90% of *baf-1*(*RNAi*) nuclei imaged ($n = 113$). However, there was no obvious pattern to the condensation defects. Clumpy condensed chromatin was either nuclear envelope-associated (Fig. 4*B*, arrows), or intranuclear (Fig. 7*A*), or both (Fig. 7*B*). The condensation status of the remaining chromatin appeared similar to bridged chromatin (Fig. 4*B Right*, asterisk). We concluded that Ce-BAF mediates changes in chromatin structure required for nuclear assembly, and chromatin capture by the nascent nuclear envelope.

Embryos That Survive *baf-1*(*RNAi*) Treatment Have DTC Migration Defects and Are Infertile. Under conditions of incomplete RNA interference, 52% of embryos escaped embryonic arrest and

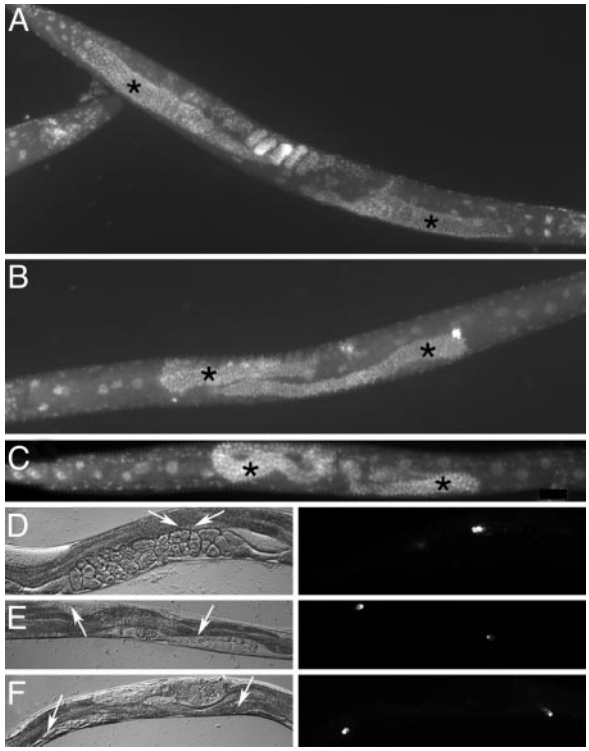

Fig. 5. Gonad morphology and DTC migration phenotypes of worms that survived *baf-1*(*RNAi*) treatment. (*A*) DAPI-stained adult worms hatched from embryos of mothers fed empty L4440 vector. Gonads are marked by asterisks. (*B* and *C*) Two DAPI-stained adult worms hatched from surviving embryos of *baf-1*(*RNAi*)-treated mothers. Gonads, marked by asterisks, are small and misplaced. (*D*) Adult worm hatched from control embryos of strain JK2049 mothers fed empty L4440 vector, imaged by DIC (*Left*) and GFP fluorescence (*Right*); GFP marks DTCs. (*E* and *F*) Two adult worms hatched from *baf-1*(*RNAi*)-treated JK2049 mothers, imaged by DIC (*Left*) and GFP fluorescence (*Right*). (*D-F*) Arrows in the DIC images indicate DTCs that are abnormally positioned in *E* and *F*, or positioned normally in *D*.

continued to develop through larval life. As adults, many of these escapers had small or misplaced gonads. Of 99 *baf-1*(*RNAi*) escapers analyzed, 12% died prematurely with a burst phenotype in which the intestines or gonads (or both) were externalized, 52% were sterile with small or misplaced gonads (Fig. 5 *B* and *C*, each gonad arm is marked by an asterisk), 10% had the bag-of-worms phenotype in which embryos hatch internally and kill the mother, and 26% laid embryos. In control embryos treated with empty L4440 vector, gonad morphology was normal (Fig. 5*A*), and viable embryos were produced by 97% of adults ($n = 104$); the other phenotypes were rare (≈1% burst, 1% bag of worms, and 1% sterile). We concluded that small reductions in Ce-BAF were not lethal during embryogenesis, but later affected gonad development. The gonad phenotypes suggested possible disruption of many cell types, potentially including DTCs that guide the developing gonad, or interacting tissues. To specifically test DTC function we down-regulated *baf-1* in worms that express GFP under the control of the *lag-2* promoter (strain jk2049), which marks DTCs (21). DTCs usually direct migration in three stages: first, away from the midbody, then, up (ventral to dorsal), and finally, back toward the midbody (22). Escapers were examined 1 week after hatching. In adults hatched from mothers fed the empty L4440 vector, both DTCs were positioned in the midbody of the worm ($n = 22$; Fig. 5*D*, arrows). In contrast, DTCs localized incorrectly in 75% of *baf-1*(*RNAi*) survivors ($n = 20$), as indicated by the arrows in the DIC image and corresponding GFP signals at right (Fig. 5 *E* and *F*). We concluded that slight reductions in Ce-BAF were not lethal, but disrupted DTC migration either directly or indirectly. Potential defects in other cell types remain to be investigated.

Discussion

Ce-lamin and three nuclear membrane proteins (Ce-emerin, Ce-MAN1, and matefin) failed to assemble properly in Ce-BAF-depleted cells, strongly supporting mutually dependent structural roles for BAF, lamins, and LEM-domain proteins during postmitotic nuclear assembly. Early embryos rely on maternally supplied proteins and mRNAs to progress through embryogenesis. Because the chromatin and mitotic phenotypes were visible as early as the two-cell stage, we conclude that Ce-BAF has direct structural roles required for efficient chromosome segregation, mitotic progression, and nuclear assembly. Down-regulation of Ce-BAF ultimately caused embryonic death at the ≈100 cell stage (gastrulation), the same stage of arrest caused by null mutations in RNA polymerase II (*ana-1*), or by soaking embryos in the potent polymerase II inhibitor, α-amanitin (23). The timing of *baf-1*(*RNAi*) lethality is therefore consistent with, but does not prove, essential roles for Ce-BAF in embryonic gene expression. The gonad phenotypes seen in *baf-1*(*RNAi*) escapers also support roles for Ce-BAF in gene expression. We assume these embryos escaped embryonic lethality by developing before or after RNAi down-regulation took effect or reached maximal efficiency. Gonad phenotypes can be caused by many different mechanisms, including defective migration of DTCs that guide each arm of the developing U-shaped gonad. DTC migration involves integrins (24) and is regulated by netrin-dependent and -independent guidance systems secreted by both the muscle cells and DTCs (25). We hypothesize that sterile *baf-1*(*RNAi*) escapers had enough Ce-BAF to get through mitosis and survive development, but experienced mild reductions in Ce-BAF that later disrupted tissue-specific gene expression. BAF is known to regulate gene expression in mammalian retinal cells: BAF binds directly to Crx and related homeodomain transcription activators, and blocks Crx-dependent gene expression *in vivo* (7). Interestingly, BAF also binds directly *in vitro* to Otx2 (7), a transcription factor that directly regulates genes encoding adhesion molecules and secreted signaling proteins involved in morphogenetic cell movements (26, 27). We therefore speculate that *baf-1*(*RNAi*) escapers are likely to have additional (potentially subtle) tissue-specific phenotypes not detected in this study.

Our mitotic findings are consistent with previous studies that used dominant-negative strategies to study BAF. The chromosome condensation defects and nuclear assembly arrest are consistent with studies in *Xenopus* nuclear assembly extracts, where exogenous BAF promoted either chromatin decondensation and nuclear growth (when added in low excess) or the opposite, chromatin hypercondensation and nuclear assembly arrest (when added in high excess) (28). Our results are also consistent with human cell studies, where postmitotic recruitment of emerin and A-type lamins into assembling nuclear envelopes was disrupted by a dominant-negative BAF mutant (29).

The genetic null phenotype for BAF was previously reported in *Drosophila melanogaster*, based on deletions that removed the entire D-BAF coding sequence (30). Genetic null phenotypes, even for essential genes, are not revealed in *Drosophila* until the larval-pupal transition, when maternally contributed mRNAs and proteins are finally depleted. Loss of D-BAF caused defects in chromatin organization and the appearance of heterochromatin-like clumps of chromatin, similar to our findings in early *C. elegans* embryos down-regulated for Ce-BAF. Other structural phenotypes in BAF-null *Drosophila* included abnormal distribution of lamin B and abnormal nuclear shapes in interphase cells (30). In contrast, neither anaphase-bridged chroma-

tin nor gapped nuclear envelopes were reported, probably because BAF-deficient *Drosophila* cells failed to enter mitosis. Notably, loss of D-BAF correlated with reduced expression of cyclins A, B, and E, and reduced entry into S phase, strongly suggesting that loss of D-BAF disrupts the expression of genes required for cell-cycle progression (30).

The similarities between the worm and fly phenotypes support the hypothesis that BAF has conserved roles in chromatin organization during interphase and nuclear assembly. Importantly, the differences reveal the range of functions that require BAF, and highlight the complementarity of RNAi and genetic null strategies. The RNAi method caused the relatively rapid depletion of Ce-BAF from early embryos, exposing mitotic phenotypes. Early embryos have only S and M phases of the cell cycle, and divide extraordinarily rapidly. Early embryos are also relatively insensitive to conditions that would normally trigger checkpoints, because of their large volume of cytoplasm relative to nuclei (31, 32). We think this is the reason why cell division can continue in Ce-BAF-depleted cells. Later in development, when embryonic gene expression begins in earnest and cells acquire both G_1 and G_2 phases of the cell cycle, phenotypes involving other BAF-dependent functions, including gene expression, would be exposed. It may be highly significant that under somatic cell-cycle conditions BAF-null *Drosophila* embryos arrest in G_1 with significantly reduced levels of G_1 (and other) cyclins (30). In summary, we suggest that the phenotype of BAF-null *Drosophila* embryos reflects primarily the loss of chromatin- or gene-regulatory functions of BAF required for progression into S phase, whereas the down-regulation phenotype in *C. elegans* early embryos reveals BAF's structural roles in mitosis and nuclear assembly.

Our results strongly suggest that Ce-BAF (*i*) mediates changes in chromatin structure during mitosis and nuclear assembly, and (*ii*) is required for LEM-domain proteins and lamins to coassemble at the chromatin surface. Our result also suggests that Ce-BAF might structurally link chromosome segregation to nuclear envelope assembly. We propose that coassembly of Ce-BAF and its partners (Ce-lamin and LEM-domain proteins) somehow stabilizes segregating chromosomes by promoting their capture by (attachment to) the nascent nuclear envelope. Consistent with this model, mouse cells with mutated lamin B1 have chromosome segregation defects and are polyploid (33). Further supporting this model, human BAF colocalizes with LAP2α on telomeres during anaphase (34) and subsequently forms transiently stable core structures at the leading and lagging faces of segregating chromatin (29, 34). Core structures persist for only 4–6 min and appear to recruit and concentrate certain nuclear membrane proteins (e.g., emerin) while excluding others (e.g., LBR) early in nuclear envelope assembly. LAP2α then disperses into the nuclear interior, whereas membrane proteins and lamins disperse along the nuclear envelope. In this light, our *C. elegans* phenotypes are consistent with the idea that Ce-BAF might normally stabilize telomere-associated core structure(s) responsible for capturing newly segregated chromatin within the nascent nuclear envelope.

We thank E. Neufeld and N. Feinstein for assistance with thin-section EM analysis; J. Austin for strains; and G. Seydoux, J. Pellettieri, A. Cuenca, and K. K. Lee for assistance with early phases of this work. We thank K. Liu, J. Holaska, K. Tifft, and M. Mansharamani for comments on the manuscript. We also thank the *C. elegans* Genetic Center, which is funded by the National Institutes of Health National Center for Research Resources, for strains. This work was supported by the USA–Israel Binational Science Foundation, the Cooperation Program in Cancer Research of the Deutsches Krebsforschungszentrum, Israel's Ministry of Science and Technology, the Israeli Science Foundation and Israel Ministry of Health (Y.G.), and National Institutes of Health Grant RO1 GM64535 (to K.L.W.).

1. Lee, M. S. & Craigie, R. (1998) *Proc. Natl. Acad. Sci. USA* **95,** 1528–1533.
2. Segura-Totten, M. & Wilson, K. L. (2004) *Trends Cell Biol.* **14,** 261–266.
3. Lee, K. K. & Wilson, K. L. (2004) *Symp. Soc. Exp. Biol.* **56,** 329–339.
4. Furukawa, K. (1999) *J. Cell Sci.* **112,** 2485–2492.
5. Cai, M., Huang, Y., Ghirlando, R., Wilson, K. L., Craigie, R. & Clore, G. M. (2001) *EMBO J.* **20,** 4399–4407.
6. Gruenbaum, Y., Margalit, A., Goldman, R. D., Shumaker, D. K. & Wilson, K. L. (2005) *Nat. Rev. Mol. Cell Biol.* **6,** 21–31.
7. Wang, X., Xu, S., Rivolta, C., Li, L. Y., Peng, G. H., Swain, P. K., Sung, C. H., Swaroop, A., Berson, E. L., Dryja, T. P. & Chen, S. (2002) *J. Biol. Chem.* **277,** 43288–43300.
8. Holaska, J. M., Lee, K. K., Kowalski, A. K. & Wilson, K. L. (2003) *J. Biol. Chem.* **278,** 6969–6975.
9. Goldman, R. D., Gruenbaum, Y., Moir, R. D., Shumaker, D. K. & Spann, T. P. (2002) *Genes Dev.* **16,** 533–547.
10. Foisner, R. (2003) *Sci. World J.* **3,** 1–20.
11. Shimi, T., Koujin, T., Segura-Totten, M., Wilson, K. L., Haraguchi, T. & Hiraoka, Y. (2004) *J. Struct. Biol.* **147,** 31–41.
12. Lee, K. K., Gruenbaum, Y., Spann, P., Liu, J. & Wilson, K. L. (2000) *Mol. Biol. Cell* **11,** 3089–3099.
13. Gruenbaum, Y., Lee, K. K., Liu, J., Cohen, M. & Wilson, K. L. (2002) *J. Cell Sci.* **115,** 923–929.
14. Liu, J., Rolef-Ben Shahar, T., Riemer, D., Spann, P., Treinin, M., Weber, K., Fire, A. & Gruenbaum, Y. (2000) *Mol. Biol. Cell* **11,** 3937–3947.
15. Liu, J., Lee, K. K., Segura-Totten, M., Neufeld, E., Wilson, K. L. & Gruenbaum, Y. (2003) *Proc. Natl. Acad. Sci. USA* **100,** 4598–4603.
16. Zheng, R., Ghirlando, R., Lee, M. S., Mizuuchi, K., Krause, M. & Craigie, R. (2000) *Proc. Natl. Acad. Sci. USA* **97,** 8997–9002.
17. Brenner, S. (1974) *Genetics* **77,** 71–94.
18. Fridkin, A., Mills, E., Margalit, A., Neufeld, E., Lee, K. K., Feinstein, N., Cohen, M., Wilson, K. L. & Gruenbaum, Y. (2004) *Proc. Natl. Acad. Sci. USA* **101,** 6987–6992.
19. Cohen, M., Tzur, Y. B., Neufeld, E., Feinstein, N., Delannoy, M. R., Wilson, K. L. & Gruenbaum, Y. (2002) *J. Struct. Biol.* **140,** 232–240.
20. Praitis, V., Casey, E., Collar, D. & Austin, J. (2001) *Genetics* **157,** 1217–1226.
21. Henderson, S. T., Gao, D., Christensen, S. & Kimble, J. (1997) *Mol. Cell. Biol.* **8,** 1751–1762.
22. Merz, D. C., Alves, G., Kawano, T., Zheng, H. & Culotti, J. G. (2003) *Dev. Biol.* **256,** 173–186.
23. Powell-Coffman, J. A., Knight, J. & Wood, W. B. (1996) *Dev. Biol.* **178,** 472–483.
24. Lee, M., Cram, E. J., Shen, B. & Schwarzbauer, J. E. (2001) *J. Biol. Chem.* **276,** 36404–36410.
25. Nishiwaki, K., Kubota, Y., Chigira, Y., Roy, S. K., Suzuki, M., Schvarzstein, M., Jigami, Y., Hisamoto, N. & Matsumoto, K. (2004) *Nat. Cell Biol.* **6,** 31–37.
26. Boncinelli, E. & Morgan, R. (2001) *Trends Genet.* **17,** 633–636.
27. Kenyon, K. L., Zaghloul, N. & Moody, S. A. (2001) *Dev. Biol.* **240,** 77–91.
28. Segura-Totten, M., Kowalski, A. K., Craigie, R. & Wilson, K. L. (2002) *J. Cell Biol.* **158,** 475–485.
29. Haraguchi, T., Koujin, T., Segura-Totten, M., Lee, K. K., Matsuoka, Y., Yoneda, Y., Wilson, K. L. & Hiraoka, Y. (2001) *J. Cell Sci.* **114,** 4575–4585.
30. Furukawa, K., Sugiyama, S., Osouda, S., Goto, H., Inagaki, M., Horigome, T., Omata, S., McConnell, M., Fisher, P. A. & Nishida, Y. (2003) *J. Cell Sci.* **116,** 3811–3823.
31. Newport, J. & Kirschner, M. (1982) *Cell* **30,** 687–696.
32. Petrus, M. J., Wilhelm, D. E., Murakami, M., Kappas, N. C., Carter, A. D., Wroble, B. N. & Sible, J. C. (2004) *Cell Cycle* **3,** 212–217.
33. Vergnes, L., Péterfy, M., Bergo, M. O., Young, S. G. & Reue, K. (2004) *Proc. Natl. Acad. Sci. USA* **101,** 10428–10433.
34. Dechat, T., Gajewski, A., Korbei, B., Gerlich, D., Daigle, N., Haraguchi, T., Furukawa, K., Ellenberg, J. & Foisner, R. (2004) *J. Cell Sci.* **117,** 6117–6128.